MBE growth of InAs/GaAs quantum dots on sintered porous silicon substrate with high optical quality in the 1.3 μ m band

Mansour Aouassa[1,2*], Giorgia Franzò[3], Elie Assaf[4], Larbi Sfaxi[2], Ridha M'Ghaieth[2] and Hassen Maaref[2]

[1]Physics Department, Faculty of Sciences and Arts, Jouf University, Jouf, Saudi Arabia.
[2]Laboratory of Micro-Opto-electronic and Nanostructures (LMON), Department of physics, Faculty of sciences, 5019 Monastir, Tunisia.
[3]CNR-IMM, via S. Sofia 64, 95123 Catania, Italy.
[4]IM2NP–CNRS–AMU, Campus de St Jérôme Case 142–F - 13397 Marseille, France.

**Corresponding author: mansour.aouassa@yahoo.fr*

Abstract

We report self-assembled InAs/GaAs quantum dots (QDs) monolithically grown on a compliant transferable silicon nanomembrane. The transferable silicon nanomembrane with flat continuous crystalline silicon layer formed via in-situ porous silicon sintering is considered a low cost seed for hetero-epitaxy of free-standing single crystalline foils for photovoltaic cells. In this paper, the compliant feature of transferable silicon nanomembrane has been exploited for direct growth of high quality InAs/GaAs (QDs) by Molecular Beam Epitaxy (MBE). Bright 1.3 µm room temperature photoluminescence from InAs/GaAs QDs has been obtained. The excellent structural and optical qualities of the obtained InAs/GaAs quantum dots offers great opportunities for realizing a low cost and large scale integration of III-V based optoelectronic device on silicon.

Introduction

Integration of III-V semiconductor nanostructures on Si substrates for optical communication and photovoltaic applications represents a very promising way towards low cost and high performance opto-electronic devices [1-3]. Currently, the fabrication technology of optoelectronic components based on semiconductor integrated on silicon appears more mature due to the advancement of epitaxial growth techniques [4]. The monolithic integration of III-V

nanostructures on silicon by direct epitaxial growth reduces the manufacturing cost of optoelectronic components and improves the performance. But the heteroepitaxy III-V semiconductor on silicon remain extremely difficult because of the high lattice mismatch and the presence of antiphase domains [5-7]. The recent success of the fabrication of 1.3 micron high-performance quantum dot lasers and high efficiency solar cells based on InAs / GaAs quantum dots directly grown on a Si substrate by molecular beam epitaxy (MBE) has increased the interest for the development of epitaxial optoelectronic devices on Si [2, 8]. The reason is that quantum dots have the least non-radiative defects compared to those in quantum wells, which improves the performance of lasers and solar cells [9]. So far, most of these III-V quantum dots have been exclusively epitaxialy grown on nominal Si substrates although there is the possibility of using other compliant substrates which are widely develop for the heteroepitaxial growth of IV-IV semiconductors films such as sintered porous silicon which is used as seed for homo-epitaxy to producing a transferrable monocrystalline silicon foils for low cost solar cells and optoelectronic devices [10-13]. Recently we have demonstrate that the stress of heteroepitaxial thin films can be accommodated by the sintered porous silicon substrates to growth of planar and free-defects crystalline semiconductors nanomembranes. We have shown that the stress driven structural evolution leading to the formation of the crystalline defects commonly observed on nominal Si (001) is fully inhibited when growing heteroepitaxial SiGe layer on such a Sintered PS substrate. The high elasticity of porous silicon is due to two characteristics: it is tensily strained and softer than bulk Si [14-17]. The tensile strain in the porous silicon layer makes it a promising compliant substrate for heteroepitaxy of perfect flat layers free of misfit dislocations for optoelectronic devices [17].

In this paper, we move forward to explore the compliant nature of sintered PSi layers for the integration of InAs/GaAs quantum dots on large scale silicon template using Molecular Beam Epitaxy (MBE) reactor.

In addition to the advantage of the compliant nature of the Sintered PS which allows easy to direct hetero-epitaxial growth of InAs/GaAs QDs on silicon substrate in contrary to the nominal Si substrate, transferring the large scale epitaxial active InAs/GaAs QDs layer to another low-cost substrates such glass substrate and keep the original substrate for reuse is also possible via using the process of layer transfer which used in industrial manufacturing of silicon solar cells [18], in this case the low porosity layer can be used as compliant layer for epitaxial growth of the active thin films and the high porosity layer serves for the layer detachment. In this layer transfer process based on Sintered PSi, the porous silicon with two layers, one with low porosity at the top and the second with high porosity at the bottom is formed on a p-type silicon substrate by electrochemical etching and is sintered via in-situ annealing at high temperature under hydrogen gas; the process of the layer transfer is schematically presented in Figure 1. During the sintering of porous silicon double-layer via heating process, the pores of the bottom high-porosity layer transforms into like-sponge layer which serves for the detachment of the active layer from the initial substrate after the epitaxial growth step. The low porosity layer can be used as a compliant layer for heteroepitaxial growth of thin films after surface smoothening via sintering process [17].

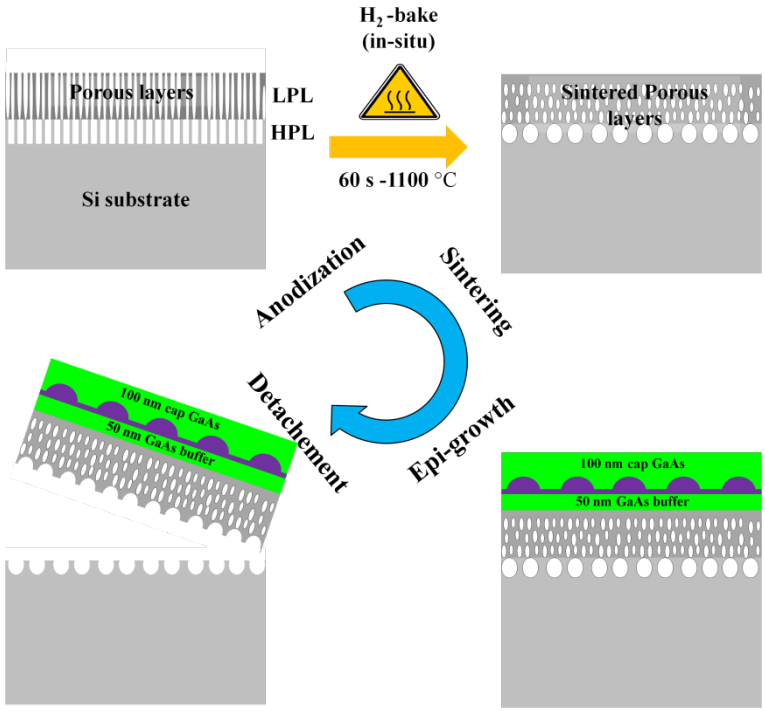

Fig. 1: Schematic view of the proposed PSi-based layer-transfer process for Large-Area Thin-Film Free-Standing InAs/GaAs QDs-on-silicon Solar Cells.

Experimental details

The porous silicon double-layer substrate is prepared via electrochemical anodizing of (100)-oriented p-type Si wafer with low resistivity (0.01 Ω cm−1) in a 35%-HF solution. After forming the first 400 nm thick low-porosity porous silicon layer, we increase the current density from 10 to 80 mA cm^{-2} to form the second 7 micron thick low-porosity porous silicon layer below the first porous layer to obtain a double layer porous silicon substrate.

Then the porous silicon sample was sintered at solid phase via in-situ heating at high temperature 1100 °C for 30 s in hydrogen ambient using ultra-high vacuum chemical vapor deposition (UHVCVD) reactor to transforms the top low-porosity porous layer into flat continuous single crystalline layer free of pores which is adequate for crystalline growth. After high-temperature sintering step, the sample of sintered PSi undergo a wet chemical cleaning using a modified Shiraki cleaning procedure for porous silicon and a second thermal cleaning via out gassing process at high temperature (760°C). The thermal cleaning was performed in

ultra high vacuum chamber with a pressure of 10^{-9} Torr to remove the volatile compounds that can be exist on the surface before the epitaxial growth of InAs/GaAs quantum dots.

Second we grow 40 nm GaAs on the sintered PSi/Si substrate at 580°C using Riber type Molecular Beam Epitaxy (MBE), then 3 Monolayers of InAs are grown at 500 °C to forms InAs qumtum dots via Stranski-Krastanov mode. During the growth process of GaAs layer of InAs quantum dots, the changes of the sample morphology was followed in real time using reflection high-energy electron diffraction (RHEED).

The morphological characterization of the sintered porous silicon substrate and the InAs QDs were investigated using Atomic Force Microscopy (AFM) operated in tapping mode and Scanning Electron Microscopy (SEM).Transmission Electron Microscopy (TEM) investigations were performed using a Jeol 2000FX operating at 250 keV to analyze the structural properties of Sintered Porous silicon substrates and InAs QDs. The PL spectra were observed using the 496,5 nm line of an Ar-ion laser. Room temperature (RT) Raman measurements were carried out using the Horiba Lab Ram ARAMIS type micro-Raman system operated with Nd:YAG laser emitting at 473 nm and coupled in a microscope through an optical fiber preserving the polarization specific to the laser wavelength and collimated throuth an achromatic lens. The laser beam was focused on the sample using an (100×/0.9 NA) objective.

Results

Figure (2-a) shows the SEM image of the as-etched porous silicon: the tiny pores and the Si nanocrystallites in the porous layer are clearly visible. Figure (2-c) inset shows the pattern of selected area electron diffraction (SAED) which confirms the perfect crystallinity present in the sintered PSi layer. Figure (2-d) shows the SEM image taken at 45° tilt for sintered PSi top layer illustrating the perfect flatness of the continuous emerging silicon nanomembrane formed at the top of sintered PSi substrate. The high qualities of the structural and morphological properties

of sintered PSi substrate, so their compliant nature, makes it a suitable substrate for epitaxial growth of high performance photovoltaic cells and optoelectronic devices.

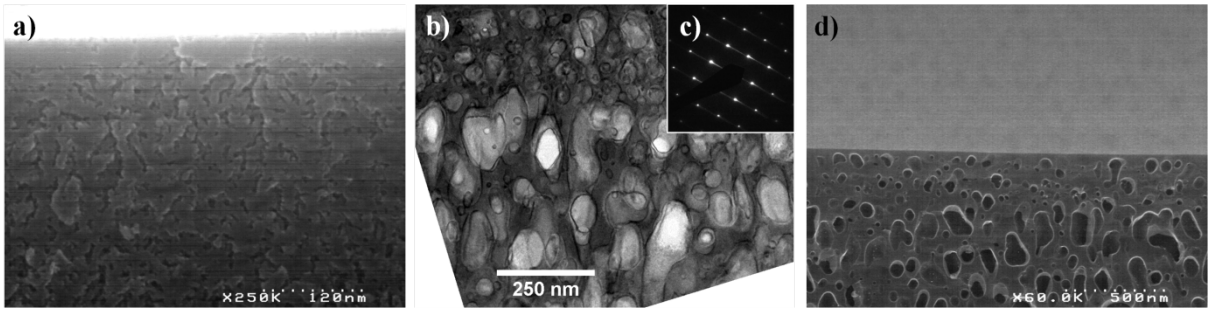

Fig. 2: (a) SEM image of as-etched porous silicon; (b) TEM cross-section image of Sintered PSi layer obtained after in-situ sintering step ; (c) electronic diffraction pattern exhibiting the crystallinity of the Sintered PSi layer; (d) SEM image taken at 45° tilt for Sintered PSi top layer showing the high flatness of the surface (d).

Figure (3) shows Reflection High Energy Electron Diffraction (RHEED) patterns captured during the growth process. The pattern changed from a streaky (Figure 3a) during the GaAs deposition, which is characteristic of 2D growth mode, to a spotty pattern (Figure 3b) after the deposition of 3 monolayers of InAs material at 500 °C. The transition from 2D to 3D growth mode which testifying the quantum dots formation was observed by the changes in the RHEED diffraction patterns.

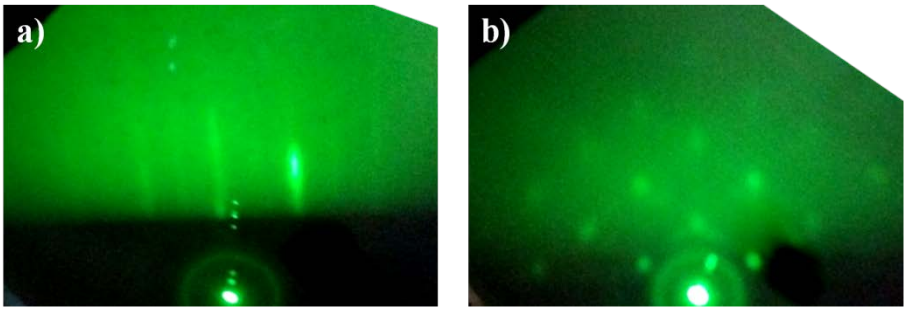

Fig. 3: RHEED diffraction patterns (a) during the growth of GaAs and (b) after the deposition of the InAs QDs.

AFM investigations of the surface morphologies of the uncapped samples were performed by AFM microscopy operated in tapping mode to reveal the size, density, and distribution of the InAs QDs. As shown in Figure 4(a), InAs QDs have been randomly formed on large scale GaAs/Sintered PSi template, with high density of 4.2 10^{10} cm^{-2}.

Figure 4-b shows the histogram of InAs QDs heights, the shape of the histogram curve reveals that two families of QDs with different sizes are formed in the sample; the large InAs QDs have an average size of (4±1) nm and low density, while the small InAs QDs have an average size of (2.5±0.5) nm and high density.

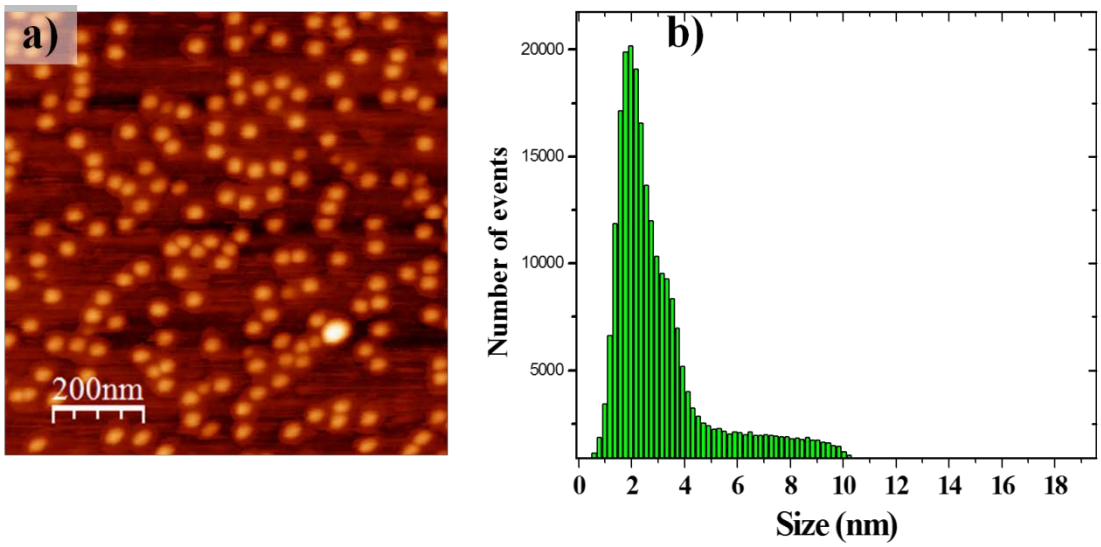

Fig. 4: (a) 2µm x *2µm AFM image of the InAs QDs grown on the GaAs/Sintered PSi template. (b) Histogram of QD height showing Gaussian distribution of InAs QDs.*

Figures 5(a) and 5(b) show respectively the cross sectional TEM images of InAs QDs grown on GaAs/Sintered PSi captured at low magnification and at high magnification. The TEM characterization reveals the presence of InAs QDs layer grown on flat GaAs / Sintered PSi, and also the successful directly growth of the GaAs buffer on Sintered PSi with homogeneous thickness and atomically abrupt GaAs/Sintered PSi interface by depositing only 40 nm of GaAs matter.

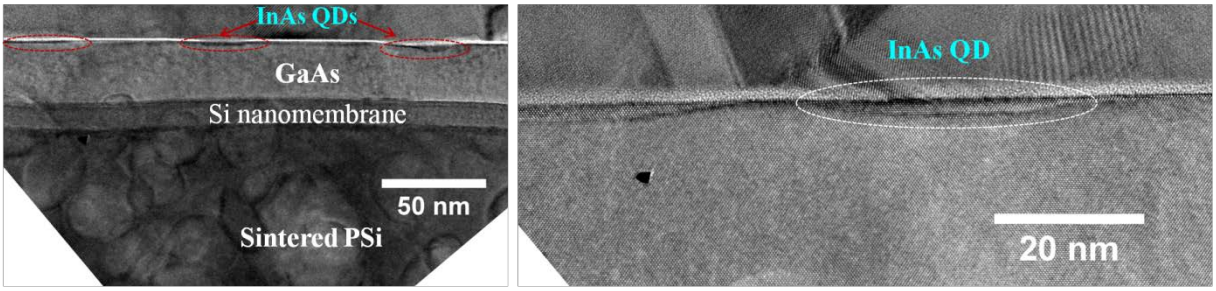

Fig. 5 (a) and 5 (b) shows respectively low magnification and high magnification cross-sectional TEM images of the QDs structure grown on the GaAs/Sintered PSi template,

These morphological and structural results clearly demonstrate that it is possible to exploit the compliant effect of porous silicon to directly grow InAs/GaAs QDs structures on a low cost template-based porous silicon, via the growth of only a few ten nanometers of GaAs buffer, contrary to the methods recently used for the direct growth of InAs/GaAs QDs on silicon templates, that requires the use of a thick GaAs layer to progressively plastically relax the mismatch stress. In addition to the compliant nature of the new proposed Sintred PSi substrate, it allows to fabricate large-area free-standing monocrystalline InAs/GaAs QDs foils for solar cells via application of the layer transfer process on the structure [18].

To support our morphological and structural data, we performed Raman measurements at room temperature to investigate the vibrational properties of the InAs/GaAs quantum dots grown on Sintered PSi substrate. Fig. 6 shows the typical Raman spectrum of InAs/GaAs QDs. There are two peaks related to the GaAs buffer layer, one at 290 cm^{-1} caused by scattering of LO phonons and the other at 265 cm^{-1} due to scattering of TO phonons. The shift of this peak to the lower wavenumber is related to the compressive strain in the GaAs buffer caused by the residual stress generated by the mismatch between the GaAs buffer and the substrate. To the left, at 254 cm^{-1}, there is a shoulder that is due to Raman scattering of InAs QDs. The inset shows a zoom-in of the peak related to InAs/GaAs QDs: a fit with two Gaussian peaks, one centered at 256 cm^{-1} due to GaAs, and another at 265 cm^{-1} due to InAs QDs is also reported. The Raman spectrum

confirms the successful formation of high quality InAs/GaAs QDs on the compliant Sintered PSi substrate.

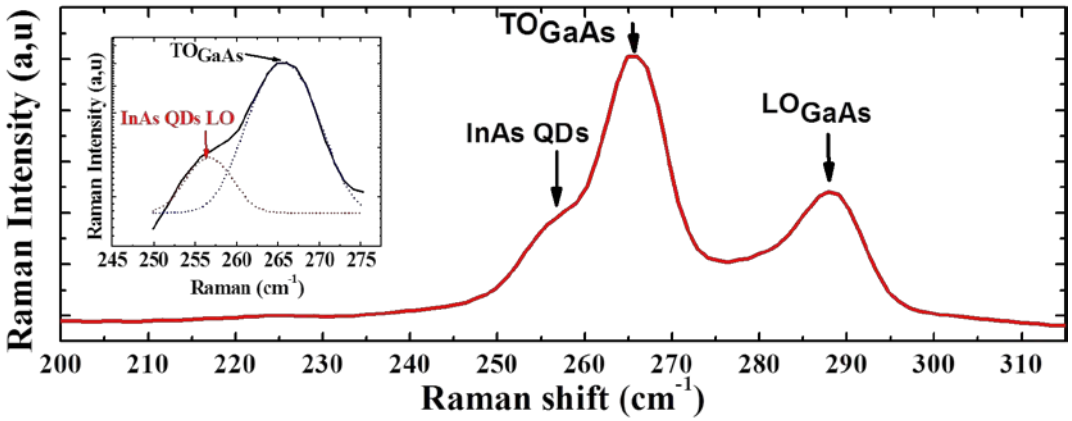

Fig. 6: Raman scattering spectra of InAs/GaAs QDs grown on Sintered PSi. The inset shows a zoom of the spectrum in the range 250-275 cm^{-1}.The fit to this peak with 2 gaussian curves is also reported.

Figure 7(a) shows that a strong photoluminescence signal in the infra-red was detected for the InAs/GaAs QDs grown on Sintered PSi at 11 K.

The high brightness of the PL emission confirms the high structural properties of the InAs/GaAs QDs formed on Sintered PSi via Stranski-Krastanov mode. The PL spectrum of InAs/GaAs QDs grown on Sintered PSi is centered at approximately 1.04 eV with multiple peaks, which can be fitted with 4 Gaussian curves centered at 0.926, 0.99, 1.053, and 1.1 eV, labeled as a–d in Fig. 7a. The resulting fitting line is also reported as a cyan dashed line. The presence of multiple peaks, which were also seen in many previous reports [19, 20], can be attributed to the step-like height fluctuation of the QDs. The change in the quantum confinement of electrons and holes from a 3 D confinement to a strong unidimensional confinement in the direction of the height caused by the decrease of the ratio of the height to the base diameter (about 50 nm) causes a big change in the band gap energy of QD InAs and the appearance of multi-peak emission. The multi-peak emission which due to the monolayer step height fluctuation of InAs quantum dots have also reported by other researcher such as Bimberg et al. [21, 22].

The result confirms the formation of high quality InAs / GaAs QDs on Sintered PSi substrates with bright photoemission in infrared similar to those obtained from the InAs / GaAs QDs grown on silicon substrate.

Fig 7(b) shows that the Photoluminescence emission of InAs/GaAs QDs grown on Sintered PSi remains strong even at room temperature. The strong PL intensity indicates the high efficiency of the InAs/GaAs QDs grown on Sintered PSi.

Measurements of temperature dependent PL have been used for studying the optical properties of InAs/GaAs QDs directly grown on Sintered PSi substrate. Fig. 7(c) displays the PL spectra measured at different temperatures in the range 11 - 300 K. From these spectra we have extracted the PL peak position and FWHM and the data are reported in Fig. 7(d).

These spectra reveal that the energy of the PL peak slightly decreases with increasing temperature, and that the PL intensities are more sensitive to non-radiative recombination. The FWHM of the PL spectrum remains slightly constant which proves the high InAs QDs uniformity. The spectrum broadening at low temperature is also increased by the additional emission of small InAs QDs. Fig. 7(e) displays the variation of the integrated Photoluminescence intensity as a function of the inverse of temperature for the InAs/GaAs QDs. The thermal activation energy given by fitting the PL quenching at high temperatures using Arrhenius equation is about 107 meV. Fig. 7(f) shows the PL peak intensity as a function of the temperature. The optical results of InAs/GaAs QDs are in good agreement with data reported in literatures [23].

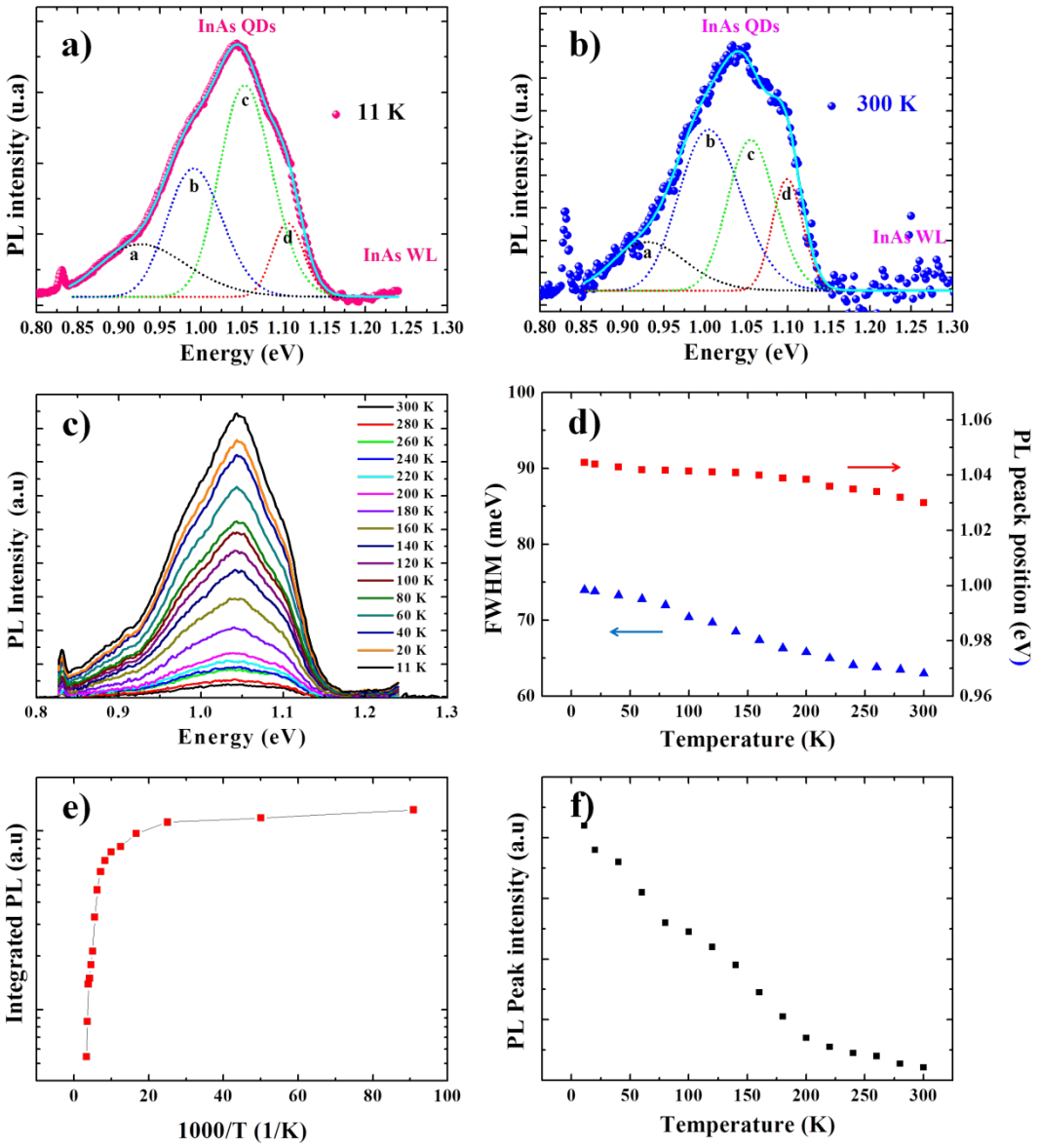

FIG. 7: PL spectra of the InAs/GaAs QDs on sinterted PSi substrate measured at 11 K (a) and at room temperature (b). Spectra have been fitted with 4 gaussian curves. PL spectra measured at different temperatures between 11 and 300 K (c); temperature dependence of the PL FWHM and peak position(d); Integrated PL intensity as a function of the inverse of the temperature(e); PL peak intensity as a function of temperature (f).

Conclusions

InAs/GaAs QDs have been successfully grown on a high quality sintered porous Si substrate by MBE. Several characterization techniques, such as Atomic Force Microscopy, Transmission Electronic Microscopy, Raman spectroscopy and photoluminescence spectroscopy are combined to probe the structural, morphological and the optical properties of novel structure of

InAs/GaAs QDs grown on sintered porous silicon. The high structural and morphological quality of the Sintered PSi substrate obtained via in-situ heating at high temperature (1100 °C for 30 s) in H_2 in ultra-high vacuum chemical vapor deposition (UHVCVD) reactor allowed the growth of promising high emissivity InAs quantum dots on transferrable porous silicon nanomembrane for low cost and high performance thin film free-standing hybrid III-V/Si devices.

References

[1] Lucas Güniat, Sara Martí-Sánchez, Oscar Garcia, Mégane Boscardin, David Vindice, Nicolas Tappy, Martin Friedl, Wonjong Kim, Mahdi Zamani, Luca Francaviglia, Akshay Balgarkashi, Jean-Baptiste Leran, Jordi Arbiol, Anna Fontcuberta , Morral; 1355833-5840. ACS Nano. (2019)

[2] Romain Cariou, Jan Benick, Frank Feldmann, Oliver Höhn, Hubert Hauser, Paul Beutel, Nasser Razek, Markus Wimplinger, Benedikt Bläsi, David Lackner, Martin Hermle, Gerald Siefer, Stefan W. Glunz, Andreas W. Bett & Frank Dimroth; volume 3, 326–333. Nature Energy. (2018)

[3] J Wu, M Tang, H Liu; Nanoscale Semiconductor Lasers. (2019)

[4] J. Seidl, J. G. Gluschke, X. Yuan, S. Naureen, N. Shahid, H. H. Tan, C. Jagadish, A. P. Micolich, P. Caroff. Regaining. 4666-4677, 19 (7). Nano Letters. (2019)

[5] Clement Merckling, Sijia Jiang, Ziyang Liu, Niamh Waldron, G Boccardi, R Rooyackers, Zhechao Wang, Bin Tian, Mariann Pantouvaki, Nadine Collaert, Joris Van Campenhout, Marc Heyns, Dries Van Thourhout, Wilfried Vandervorst and Aaron Thean;. volume 66, issue 4, 107-116 ECS Trans. (2015)

[6] Bernardette Kunert, Yves Mols, Marina Baryshniskova, Niamh Waldron, Andreas Schulze and Robert Langer; Semicond. Sci. Technol. 33 093002. (2018)

[7] A. Zhou, Y. Ping Wang, C. Cornet, Y. Léger, L. Pédesseau, V. Favre-Nicolin, G. A. Chahine, T. U. Schülli, J. Eymery, M. Bahri, L. Largeau, G. Patriarche, O. Durand and A. Létoublon. J. Appl. Cryst. 52, 809-815. (2019)

[8] Markus Feifel , Jens Ohlmann , Jan Benick , Martin Hermle, Jurgen Belz, Andreas Beyer, Kerstin Volz, Thomas Hannappel, Andreas W. Bett, David Lackner, and Frank Dimroth. IEEE Journal of Photovoltaics, 1–6. (2018)

[9] Shih-Yen LIN, Yao-Jen TSAI and Si-Chen LEE ; Jpn. J. Appl. Phys. Vol. 40 (2001) pp. L 1290–L 1292

[10] Lukianov, K. Murakami, C. Takazawa, and M. Ihara; APPLIED PHYSICS LETTERS 108, 213904 (2016)

[11] Hariharsudan, Sivaramakrishnan Radhakrishnan, Roberto Martini, Valerie Depauw, KrisVan, Nieuwenhuysena,Twan Bearda, Ivan Gordon, Jozef Szlufcik, Jef Poortmans; Solar Energy Materials and Solar Cells.Volume 135, April 2015, Pages 113-123

[12] Progress H. J. Kim, V. Depauw, G. Agostinelli, G. Beaucarne, J. Poortmans. Thin Solid Films; Volumes 511–512, 26 July 2006, Pages 411-414

[13] C. S. Solanki, L. Carnel, K. Van Nieuwenhuysen, A. Ulyashin, N. Posthuma, G. Beaucarne, y and J. Poortmans; Prog. Photovolt: Res. Appl. 2005; 13:201–208.

[14] Boucherif, N. P. Blanchard, P. Regreny, O. Marty, G. Guillot, G. Grenet, V.Lysenko; Thin Solid Films Volume 518, Issue 9, 2010, Pages 2466-2469

[15] M. Aouassa, S. Escoubas, A. Ronda, L. Favre, S. Gouder, R. Mahamdi, E. Arbaoui, A. Halimaoui, and I. Berbezier Appl. Phys. Lett. 101, 233105 (2012)

[16] Mansour Aouassa, Imen Jadli, Latifa Slimen Hassayoun, Hassen Maaref, Gerard Panczer, Luc Favre, Antoine Ronda, Isabelle Berbezier ; Superlattices and Microstructures, Volume 112, p. 493-498.12/2017

[17] Isabelle Berbezier, Jean-Noël Aqua, Mansour Aouassa, Luc Favre, Stéphanie Escoubas, Adrien Gouyé, and Antoine Ronda ; Phys. Rev. B 90, 035315 –2014

[18] C. S. Solanki; R.R. Bilyalov, J. Poortmans , R. Mertens Solar Energy Materials and Solar Cells Volume 83, Issue 1, 1 June 2004, Pages 101-113.

[19] Shigehiro Kitamura, Masaya Senshu, Toshio Katsuyama, Yuji Hino, Nobuhiko Ozaki, Shunsuke Ohkouchi, Yoshimasa Sugimoto and Richard A Hogg; Nanoscale Research Letters (2015) 10:231

[20] Hino Y, Ozaki N, Ohkouchi S, Ikeda N, Sugimoto Y. Growth of InAs/GaAs quantum dots with central emission wavelength of 1.05 μm using In-flush technique for broadband near-infrared light source. J Cryst Growth. 2013;378:01–505.

[21] Guffarth F, Heitz R, Schliwa A, Pötschke K, Bimberg D. Observation of monolayer-splitting for InAs/GaAs quantum dots. Phys E. 2004;21:326–30.

[22] Heitz R, Guffarth F, Pötschke K, Schliwa A, Bimberg D, Zakharov ND, et al. Shell-like formation of self-organized InAs/GaAs quantum dots. Phys Rev B. 2005;71(045325):1–7

[23] Yating Wan, Qiang Li, Yu Geng, Bei Shi, and Kei May Lau. Applied Physics Letters 107, 081106 (2015).